Cement & Concrete Composites 36 (2013) 121–127

Contents lists available at SciVerse ScienceDirect

Cement & Concrete Composites

journal homepage: www.elsevier.com/locate/cemconcomp

Improvement of cement-based mortars by application of photocatalytic active Ti–Zn–Al nanocomposites

T. Vulic [a,*], M. Hadnadjev-Kostic [a], O. Rudic [a], M. Radeka [b], R. Marinkovic-Neducin [a], J. Ranogajec [a]

[a] University of Novi Sad, Faculty of Technology, Bul. Cara Lazara 1, 21000 Novi Sad, Serbia
[b] University of Novi Sad, Faculty of Technical Science, Trg Dositeja Obradovica 6, 21000 Novi Sad, Serbia

ARTICLE INFO

Article history:
Received 31 January 2012
Received in revised form 23 July 2012
Accepted 24 July 2012
Available online 1 August 2012

Keywords:
Photocatalysis
Cement
Mortar
Layered double hydroxides

ABSTRACT

Photocatalytic active TiO_2 has been extensively applied in construction material science due to its ability to remove pollutants from material surfaces. New inorganic–inorganic nanocomposite photocatalyst based on layered double hydroxides (LDHs) associated to TiO_2 were introduced in order to increase the compatibility of photocatalyst with cement-based mortars. Different materials were prepared and characterized: cement paste with Ti–Zn–Al powder, mortar with cement paste finishing layer containing Ti–Zn–Al LDH and mortar with Ti–Zn–Al coatings. Degradation of methylene blue under *UV* light was selected as photocatalytic test reaction. The correlation between surface properties and photocatalytic activity was analyzed. The synergetic effect between TiO_2 and Zn–Al-LDH contributes to pronounced photocatalytic performances, improving at the same time mortar performances as an important indicator of the compatibility of photocatalyst with mortar. The photocatalyst introduction procedure influences the active sites surface concentration, giving preference to surface coating method. However, introduction of photocatalyst into the bulk, having lower photocatalytic activity, results in an overall more stable system for prolonged application.

© 2012 Elsevier Ltd. All rights reserved.

1. Introduction

Cement is one of the most used man-made substances, applied on a large scale in the production of spectra of cement-based construction materials (mortars, concrete, and renders). Extremely large surfaces of cement-based materials in build environment and infrastructural objects (buildings, industrial plants, tunnels, pavements, roads, tunnels, bridges, etc.) are exposed to changing and increasingly polluted environment, causing gradual deterioration of both surface properties and structural characteristics of different construction materials. Prolonged durability and lower costs of the maintenance of build environment surfaces is one of the main challenges in developing new construction materials of improved properties. But, even more demanding challenge is to develop new functionality of self-cleaning to the large exposed surfaces by introducing photocatalytic function to cementitious materials. In interaction with the solar light, photocatalyst promotes the decomposition of the polluting agents (organic, microbial, and inorganic) adsorbed on the surfaces or present in the surrounding air. The potential of large scale application of these value-added materials is huge particularly in most urban areas where air pollution is relatively high [1]. In recent years, the increasing interest in combining photocatalytic active materials with cementitious materials has been recognized in a number of publications [1–5] as well as in development of some commercial products [6]. Most of the published research refers to the application of nano-sized TiO_2 semiconductor as photocatalytic active material [2,7-9], mentioning also some of serious challenges which need to be approached in developing new functionality: achieving sufficient and stable photocatalytic activity in changing conditions of real environment; maintaining or even improving the key building material properties in the modified structure, especially physical and mechanical; developing of photocatalytic active material having adequate compatibility with the substrate and therefore durability in aggressive outdoor environment [1,2,10].

Referring to the cement-based materials with TiO_2 some of the reported finding pointed out that the introduction of TiO_2 modifies the properties concerning strength, abrasion, hardness, change of particle packing and the related phenomena, as well as the kinetics of hydration process [8,9,11]. Different techniques for TiO_2 application in the cement-based matrix have been used, such as: mixing with the cementitious materials, sputtering, spray coating and sol–gel dip coating [2]. It has to be underlined that technique should be carefully selected since it influences photocatalytic activity (nature and number of active sites), physico-chemical properties and stability of the surface.

* Corresponding author.
E-mail addresses: tvulic@uns.ac.rs (T. Vulic), hadnadjev@tf.uns.ac.rs (M. Hadnadjev-Kostic), ognjenrudic@tf.uns.ac.rs (O. Rudic), mirka@uns.ac.rs (M. Radeka), seka@ins.ac.rs (R. Marinkovic-Neducin), janjar@uns.ac.rs (J. Ranogajec).

0958-9465/$ - see front matter © 2012 Elsevier Ltd. All rights reserved.
http://dx.doi.org/10.1016/j.cemconcomp.2012.07.005

The main focus of this study was to increase the compatibility of the photocatalytic materials with cement-based mortars by the introduction of new inorganic–inorganic nanocomposite photocatalyst based on layered double hydroxides (LDHs) associated to TiO_2. LDHs, also known as anionic clays, were chosen due to the possibility to tailor their physical and chemical properties during synthesis and especially because LDHs and LDH-like materials represent one of the phases that form during cement hydration [12–14]. Zinc was selected as constituent LDH metal because of its photocatalytic and antimicrobial activity with the intention to possibly contribute to the overall activity of novel Ti–Zn–Al nanocomposite. In order to evaluate the photocatalytic material influence on the overall properties of the cement-based material, in the first part of the study physico-chemical properties (morphology, texture and microhardness) of the cement paste with Ti–Zn–Al nanocomposite were characterized. Based on the finding, further investigation was directed onto the mortar systems obtained by using different photocatalyst application techniques. Degradation of methylene blue under *UV* light was selected as the test reaction for the investigation of photocatalytic activity. The photocatalytic study was targeting the evaluation of overall photocatalytic efficiency and the nature of active sites present in samples with Ti–Zn–Al nanocomposite introduced either at the surface as thin coating (spray technique), or in the bulk as finishing cement paste layer. The correlation between surface properties (hydrophilicity, micro-hardness and surface roughness) and photocatalytic activity of mortar based samples was considered in order to evaluate the catalytic efficiency, compatibility with matrix and adequate technique of novel nano-sized photocatalytic material application in mortars and renders.

2. Experimental procedures

2.1. Preparation of samples

Wet impregnation of TiO_2 onto Zn–Al layer double hydroxides (LDHs) was used for the preparation of Ti–Zn–Al LDH nanocomposites. Before the impregnation process, Zn–Al LDH were synthesized by low supersaturation (LS) coprecipitation method at constant pH (9–9.5) [15]. Precursors, $Zn(NO_3)_2{\cdot}6H_2O$ and $Al(NO_3)_3{\cdot}9H_2O$ were continuously ($4\ cm^3\ min^{-1}$) added at constant temperature (40 °C) and by simultaneous addition of 0.67 M Na_2CO_3 and 2.25 M NaOH solution the pH was maintained constant. The precipitates were aged for 15 h, washed with water until pH 7, dried 24 h at 100 °C and calcined 5 h, at 500 °C in air. The wet impregnation process was carried out using the TiO_2 suspension (VP Disp. W 2730 X Degussa) that was diluted (3 mass%) in a 0.67 M Na_2CO_3 base solution and loaded onto calcined Zn–Al LDH powder. The excess water was removed in a rotary vacuum evaporator at 55 °C. The impregnated sample was dried for 12 h at 100 °C and calcined for 5 h at 500 °C after which the Ti–Zn–Al LDH nanocomposite powder was obtained. The Ti–Zn–Al LDH nanocomposite suspension that was used for coatings on mortar was prepared using sol–gel method with H_2O_2 solution [16].

Ordinary Portland cement (CEM I 42.5R – OPC) was used in order to prepare two series of cement pastes: reference cement paste (CP) and cement paste mixed with 1 mass% of Ti–Zn–Al LDH nanocomposite powder (CPC). Pastes were prepared with W/C = 0.4, casted into bars ($6 \times 1 \times 1$ cm). Referent CP samples were cured according to the procedure defined in SRPS EN 196-7:2010 standard [17], while in the case of CPC samples the procedure was modified, due to the observed delayed setting and slow hardening process, with an prolonged initial curing period (5 days of curing at 25 °C and relative humidity of 98%).

The mortars were prepared using the standard procedure (SRPS EN 196-7:2010 standard [17]). Three series of mortar based samples were prepared: reference mortar (M), mortar with a finishing layer of cement paste containing Ti–Zn–Al LDH nanocomposite (ML) and mortar with Ti–Zn–Al LDH nanocomposite coating (MC). For the preparation of ML, the CPC cement paste was applied onto the freshly prepared mortar reaching the final layer thickness of 7 mm when dried. For the preparation of MC, the Ti–Zn–Al LDH nanocomposite suspension was applied onto mortar specimens using the spay technique in the chamber. Three layers were deposited on each specimen. Conditions of the spray technique were: spraying pressure 6.5 MPa, distance spray device – specimen 90 cm, angle of spraying 45°, diameter of nozzle 1.3 mm. The standard curing conditions for both ML and MC samples were modified due to observed delayed settings and slow hardening process with prolonged initial curing period (25 °C, 5 days, relative humidity of 98%).

2.2. Testing procedures

The mechanical properties, Vickers micro-hardness (*HV*) were determined by Vickers micro-hardness technique (Microhardness tester model HVS 1000A, ZZV Precision Tool Suplly, with load of 1 N).

Surface energies were evaluated by measuring the initial contact angle between the water droplets and the surface (Surface Energy Evaluation System, Advex Instruments, Brno, Czech Republic). The water droplets of 5 μl in volume were gently deposited on the substrate surface using a micro-syringe. All measurements of the initial contact angles were performed at five different points for each of the three specimens of the prepared mortar samples.

The surface roughness measurements were performed using Surtronic 25, Taylor Hobson precision device and the data were calculated following ISO 4287 standard. The surface roughness of mortar based samples was evaluated based on *Ra* parameter which represents average roughness values obtained of a 4 mm linear probe length.

The morphology of surface and cross section of samples was assessed by Scanning Electron Microscopy, SEM, (Oxford instrument JEOL – ISM. 35).

Surface area and pore size distribution were analyzed using low-temperature nitrogen sorption at −196 °C (Micromeritics ASAP 2010 instrument). Samples were degassed at 100 °C prior to the isotherm measurements. The surface area was determined using the Brunauer–Emmet–Teller (BET) method and pore size distribution was calculated using the Barret–Joyner–Halenda (BJH) equation.

The photocatalytic behavior of mortar based samples (M, ML and MC) exposed to *UV* irradiation was investigated by monitoring

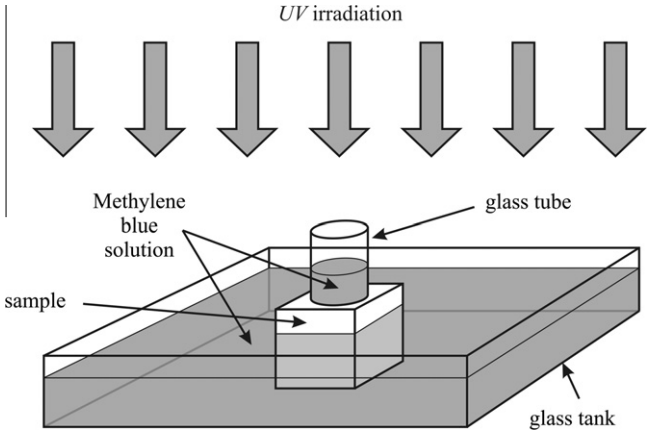

Fig. 1. Schematic of experimental set-up.

the methylene blue (MBlue) concentration change [18]. On the 28th day of curing, the samples were removed from the water and dried for 24 h at 30 °C. The samples were cut (specimen dimensions: 4 × 4 × 4 cm), a bottomless glass tube (inner diameter 33 mm, height 70 mm) was fixed with silicon on each sample specimen and filled with the 10 ppm dm^{-3} MBlue solution enabling a direct contact between the active surface of the sample and the dye. The specimens were surrounded by the same MBlue solution Fig. 1 in order to maintain constant saturation of the porous system [19].

Since the samples are porous systems and capable of liquid absorbance, a preabsorption test in MBlue solution (24 h) was carried out in order to saturate the samples before the photocatalytic experiments. After the preabsorption period, the MBlue solution was replaced by freshly prepared 10 ppm dm^{-3} MBlue solution. The samples were *UV* irradiated (EVERSUN lamp, 0.922 mW/cm^2 light intensity) for 30, 90, 150 and 210 min. The distance between the *UV*-lamp and the samples was 35 cm. In order to eliminate possible further adsorption effects, the corresponding specimens were kept in the dark and MBlue concentration was also measured at the defined time intervals. The solution within the glass tubes was used for the evaluation of the MBlue degradation. The MBlue concentration was measured by monitoring major absorption peak at $\lambda = 664$ nm using *UV–VIS* spectrophotometer (EVOLUTION 600 spectrophotometer). The photocatalytic activity of the samples was estimated by removal efficiency $A(\%) = [(C_0 - C)/C_0] \times 100$;

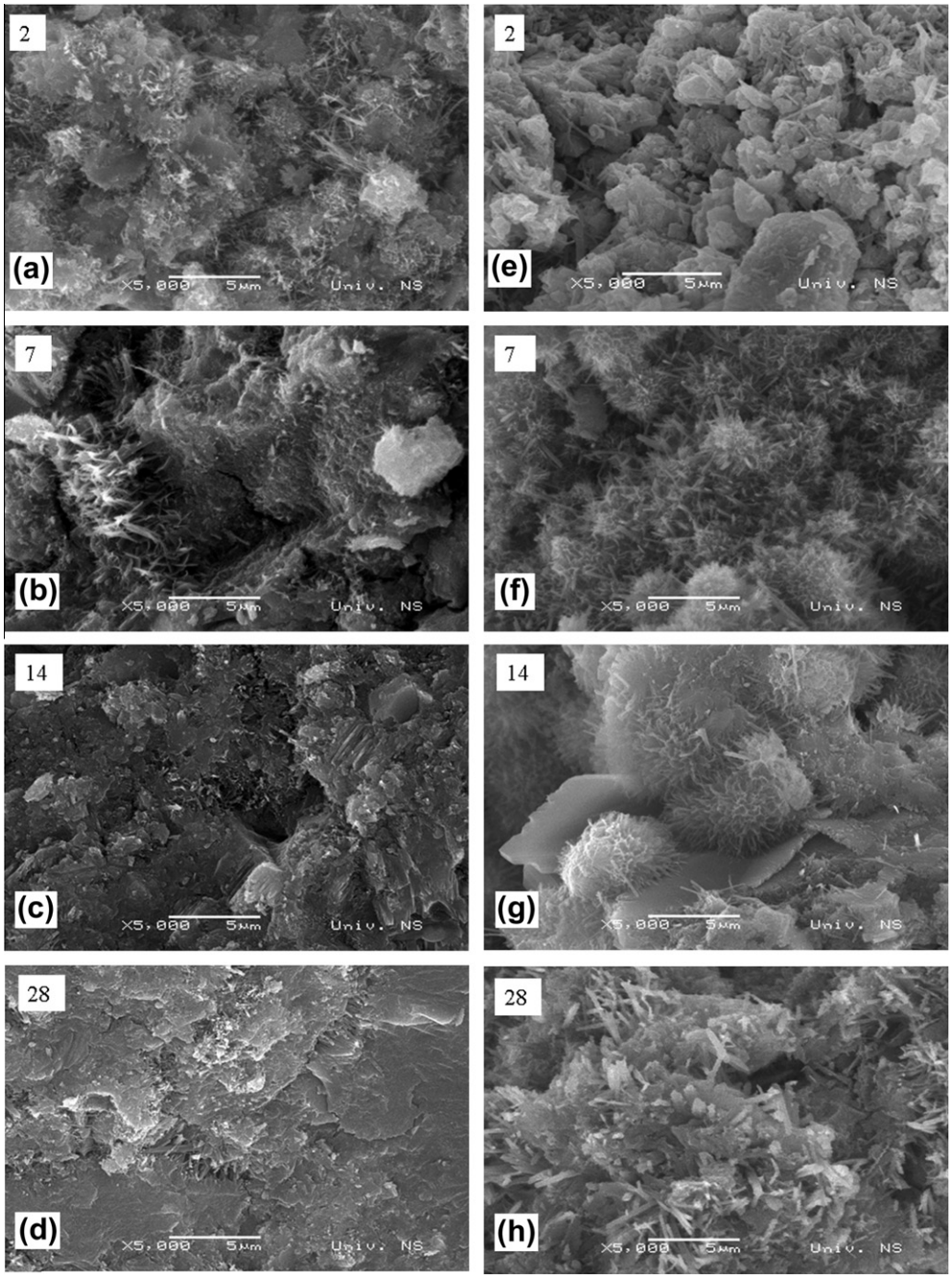

Fig. 2. Specimen cross section SEM micrographs (magnification 5000×) for different curing times: (a) CP 2 days, (b) CP 7 days, (c) CP 14 days, (d) CP 28 days, (e) CPC 2 days, (f) CPC 7 days, (g) CPC 14 days and (h) CPC 28 days.

where C_0 is the MBlue concentration of sample in the dark at the defined time, C is the MBlue concentration of sample under *UV* light at the defined time.

The photocatalytic performances of the calcined Ti–Zn–Al LDH nanocomposite powder, calcined Zn–Al LDH powder and TiO_2 powder (obtained by drying of TiO_2 suspension) were also investigated. The photocatalytic tests were performed in a Pyrex flask batch-type reactor, in the same test reaction, using the same under *UV* lamp. Catalyst powders (50 mg of Ti–Zn–Al LDH nanocomposite, 50 mg of calcined Zn–Al LDH powder and 10 mg of TiO_2 powder) were added to 100 ml of MBlue water solution (10 ppm dm^{-3}) and vigorously stirred for 30 min to establish adsorption/desorption equilibrium between the dye and the surface of the catalysts. At defined time intervals aliquots were taken and catalyst separated from the solution. Blank samples – reaction solutions with catalysts, were kept in the dark, treated the same way as irradiated samples and MBlue concentration was measured in order to eliminate possible additional adsorption phenomena. The photocatalytic activity was estimated by removal efficiency using the same formula as for the mortar based samples.

3. Results and discussion

3.1. Physico-mechanical characterization

During the preparation procedure of CPC paste, a reduced workability was observed. Possible explanation, according to literature data [20], could be that the presence of nanocomposites in cement pastes increases the need for water in order to keep the workability at the constant level. Although the workability of CP and CPC pastes were different; neither additional water nor admixture were added in order to focus just on the changes caused solely by the addition of nanocomposites. Slower hardening process was also observed for the CPC pastes after the first 24 h of curing process, since the CPC specimens demolding was not possible and initial curin period was prolonged (5 days at 25 °C and relative humidity of 98%).

The phase development during the curing process of CP and CPC samples was monitored on the specimen cross-section by SEM analysis (Fig. 2). Due to the decreased workability, the CPC structure has a much larger porosity than CP paste, Fig. 2a and e. After 7 days of curing, the CPC paste reaches similar C–S–H structure that was developed in the CP paste after only 2 days of curing, Fig. 2a and f. The observed phenomena could be a consequence of the delayed hydration process due to presence of the Zn compounds in photocatalytic material as well documented in other investigations [21,22]. In explaining the mechanism, the authors [23,24] propose that Zn interacts with the cement clinker grains, precipitates as calcium zincite at the surface, and retards setting. After a few days this compound disappears and setting process is no longer disturbed, as confirmed also by our investigation. After 14 and 28 days of CP paste curing, massive calcium hydroxide crystals, as well as poorly crystalline C–S–H hydrate with a fibrous shape were formed, Fig 2c, and 2d. The comparison of CP and CPC pastes revealed that after 7 days of curing, CPC had better distribution of the C–S–H phase (Fig. 2f); after 14 days, these phases are more pronounced in CPC paste (Fig. 2g); concluding the curing process after 28 days, the fibrous structure was detected as the dominant phase in CPC paste (Fig. 2h). A positive effect of Ti–Zn–Al nanocomposite on the crystallization rate could be explained by the presence of additional crystallization nucleuses in the system, as confirmed also by literature data from investigation of other nanoparticles effects [8,9].

The results from the micro-hardness analysis and the corresponding SEM micrographs of CPC paste surface are presented in Figs. 3 and 4. After 28 days of curing the micro-hardness is two times higher for CPC sample then for CP sample (Fig. 3). It could be concluded that the presence of Ti–Zn–Al LDH nanocomposite significantly influences surface micro-hardness probably due to a more homogenous distribution of fibrous phase and of other phases on the CPC surface. With the CPC increase in curing time; there is a noticeable change in surface phase composition as documented by SEM Fig 4.

The textural analysis of CP and CPC is presented in Fig. 5 and Table 1. The adsorption–desorption isotherms of the samples (Fig. 5a) have the same isotherm type (type IV) typical for mesoporous materials, characterized by a broad type H3 hysteresis loop confirming the presence of aggregated of plate-like particles forming a non-uniform slit-shape pores [25,26]. A multimodal pore size distribution was detected for both PC and PCP samples Fig. 5. The CPC sample has a more developed surface area and BJH desorption cumulative pore volume when compared to CP sample, Table 1. This indicates that the presence of Ti–Zn–Al nanocomposite in the cement paste influences the development of porous structure with the increased participation of smaller and larger mesopores (Fig. 5b) in comparison to the referent CP sample (Table 1), being important for the development of active photocatalytic surface. The low cumulative pore volume of CP sample, Table 1, is the consequence of the porous structure, as also confirmed by morphological analysis.

On the basis of the morphological, mechanical and textural analysis results it was concluded that the cement paste prepared with photocatalytic active Ti–Zn–Al nanocatalyst, due to its positive effects on the cement paste properties, should be further investigated in the real systems. For this reason CPC was used as the finishing layer on mortars. Photocatalytic measurements, as well as and surface and mechanical property characterization were performed on prepared mortar based samples.

Surface properties (initial contact angle, Vickers micro-hardness and Ra parameter), Table 2, and photocatalytic activity of mortar based samples were estimated after 28th day of curing. The mortar without photocatalyst (M) showed higher contact angle (lower surfaces energy) and the lowest surface roughness. The introduction of Ti–Zn–Al nanocomposite, whether into the bulk (ML) or as a coating on surface (MC), decreases the contact angle (improves the surface hydrofilicity), increases the surface roughness with some exfoliation observed when exposed to the real conditions. The highest hydrofilicity (lowest contact angle) was measured for the coated mortar (MC).

3.2. Photocatalytic activity

The photocatalytic activity of powder samples is presented in Fig. 6. The comparative investigations on the powder systems were

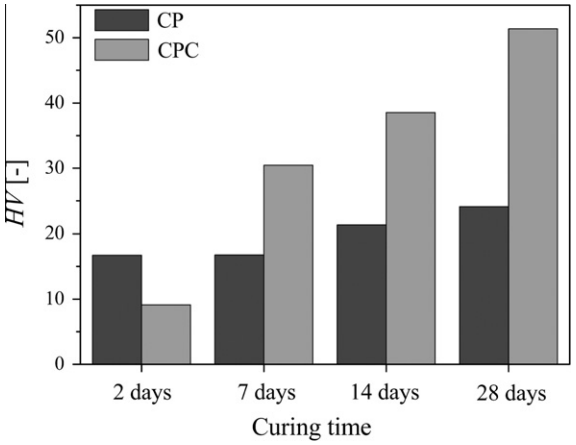

Fig. 3. The influence of curing time on micro-hardness of CP and CPC samples.

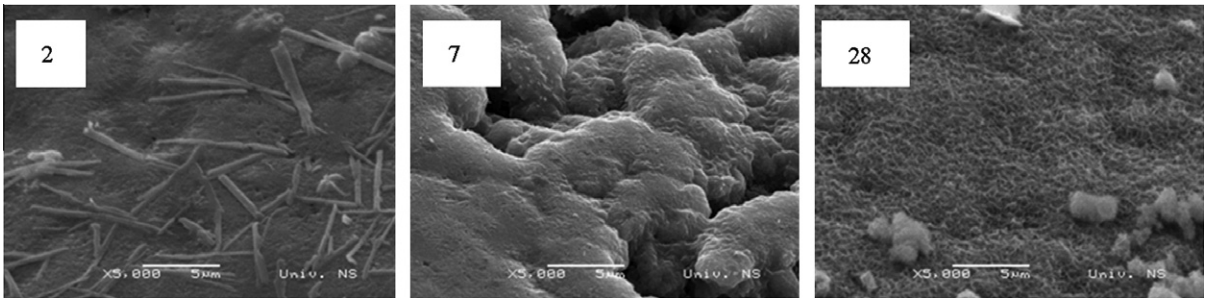

Fig. 4. SEM micrographs of CPC surface after 2, 7 and 28 days (magnification 5000×).

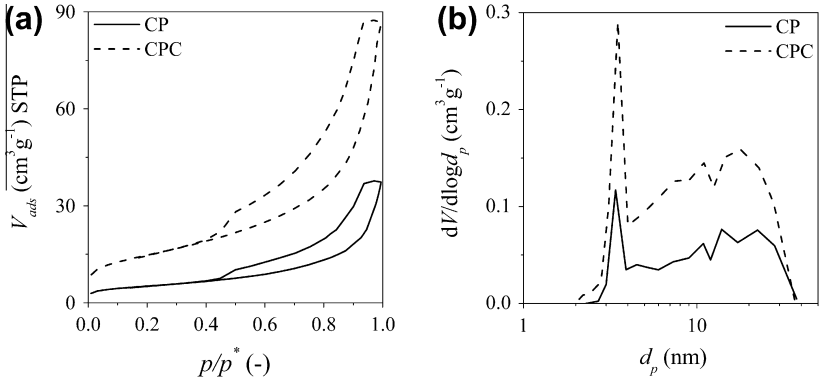

Fig. 5. Textural analysis: (a) adsorption–desorption isotherms and (b) pore size distribution of samples CP and CPC.

selected as relevant for activity comparison, since when applied in the cement paste/mortar systems some other effects could mask the essential interaction leading to synergic effect between TiO_2 and Zn–Al LDH. When TiO_2 was added to the reaction system (10 mg TiO_2 loading in the reaction chamber) 90% conversion of MBlue was reached after 60 min reaction time, leveling afterwards almost to the plateau value. When the reaction was performed in the same conditions but with 50 mg loading of Ti–Zn–Al LDH nanocomposite (3 mass%TiO_2 on Zn–Al LDH, calculated total loading of 1.46 mg TiO_2 in the reaction system), the 81% conversion was observed in the 60 min reaction period. Since the overall TiO_2 loading in the reaction was 6.8 times lowered when Ti–Zn–Al LDH nanocomposite was applied, the synergy of both composite components was identified, specially taking into account that the Zn–Al LDH alone has much lower activity under the same reaction conditions (50 mg Zn–Al LDH: 14% MBlue conversion after 60 min).

Table 1
Surface area and BJH desorption cumulative pore volume of samples CP and CPC.

Sample	Surface area ($m^2\ g^{-1}$)	BJH desorption cumulative pore volume ($cm^3\ g^{-1}$)
CP	17.91	0.0587
CPC	51.25	0.1367

Table 2
Surface properties of 28 days old mortars.

Samples	Initial contact angle (°)	*HV* (–)	*Ra* (–)
M	58.31	32.8	4.12
ML	48.22	38.9	7.82
MC	33.87	[a]	11.76

[a] Not possible to measure HV due to very rough surface.

The photocatalytic activity of samples MC, ML and M is presented in Fig. 7. Mortars with nanocomposite coatings (MCs) showed high photocatalytic activity with the removal efficiency up to 28% after 3.5 h of *UV* irradiation. The mortar with finishing layer (ML) exhibited lower activity with the removal efficiency up to 16%, whereas the referent mortar showed low removal efficiency reaching 6% after 3.5 h of *UV* irradiation. For the referent mortar (M) the MBlue removal efficiency reaches a steady-state plateau at 6% after 30 min of *UV* irradiation implying no further increase with time. Better exposure of active sites on the mortar surface, necessary for photocatalytic reaction, was achieved in the case of nanocomposite coatings (MCs) compared to the samples where nanocomposites were introduced into the mortar bulk

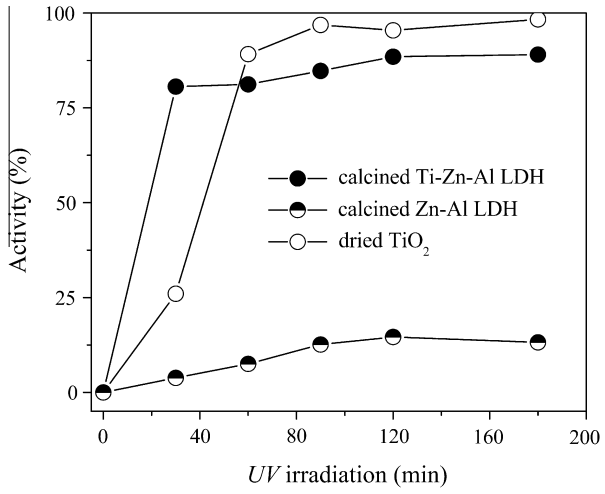

Fig. 6. Photocatalytic activity of calcined Ti–Zn–Al LDH nanocomposite powder, calcined Zn–Al-LDH powder and dried TiO_2 powder.

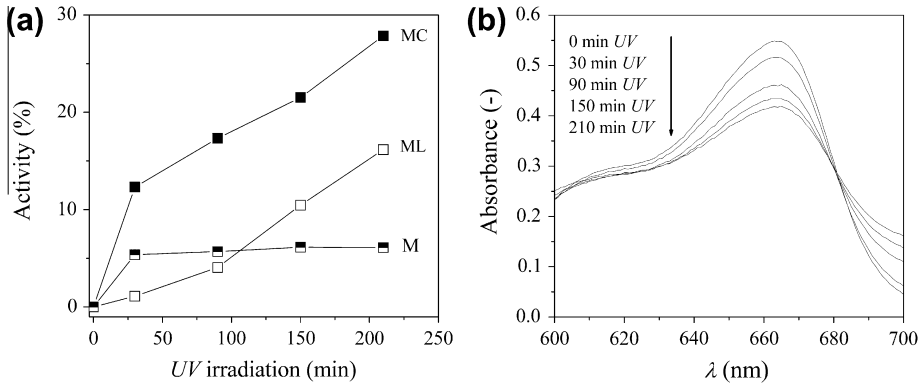

Fig. 7. Photocatalytic measurements: (a) photocatalytic activity of M, ML and MC; (b) absorbance spectra of MBlue degradation with *UV* irradiation time for MC.

(ML). The removal efficiency of both MC and ML samples did not reach a steady-state plateau within the measured *UV* irradiation time interval, indicating a further increase with time. The removal efficiency curves of ML and MC samples show almost parallel increase with time supporting the previous conclusion on the importance of surface active site concentration, but confirming also that the active sites are of the same nature, the only difference being the number of accessible sites.

4. Conclusions

The introduction of the photocatalytic active inorganic–inorganic nanocomposites to the cement-based mortars improved overall mortar properties (micro-hardness and crystallinity) bringing in the same time a new value-added photocatalytic function, as well as higher hydrofilicity, to the traditional building material. Based on comparative investigations it was concluded that the synergetic effect between TiO_2 as traditional photocatalytic semiconductor and Zn–Al-LDH contributes to the overall photocatalytic performances, improving also the compatibility of the photocatalytic active phase with the mortar matrix. The procedure of photocatalytic active component introduction influences the surface concentration of the catalytic active sites, giving the preference to surface coating method in comparison to the mortar bulk application when discussing solely the photocatalytic efficiency, but not changing the nature of active sites. However, the introduction of the catalyst active phase into the bulk, even with lower but still acceptable photocatalytic activity, results in a more stable system, concerning surface mechanical properties and C–S–H distribution. Considering the need to balance different photocatalyst performance requirements and the expected overall performances of the product, the introduction of the catalyst active phase into the bulk appears to be more promising for sustainable long-term applications.

Acknowledgments

The financial support from Serbian Ministry of Science and Technological Development (Contract No. III 45008) and from the Provincial Secretariat for Science and Technological Development of Vojvodina (Contract No. 114-451-2084/2011) is gratefully acknowledged.

References

[1] Chen J, Poon CS. Photocatalytic cementitious materials: influence of the microstructure of cement paste on photocatalytic pollution degradation. Environ Sci Technol 2009;43:8948–52.
[2] Chen J, Kou SC, Poon CS. Photocatalytic cement-based materials: comparison of nitrogen oxides and toluene removal potentials and evaluation of self-cleaning performance. Build Environ 2011;46:1827–33.
[3] Ruot B, Plassais A, Olive F, Guillot L, Bonafous L. TiO_2 – containing cement paste and mortars: measurements of the photocatalytic efficiency using rhodamine B-based colorimetric test. Solar Energy 2009;83:1794–801.
[4] Augugliario V, Loddo V, Pagliaro M, Palmisano G, Palmisano L. Clean by light irradiation. Practical applications of supported TiO_2. Cambridge: Royal Society of Chemistry; 2010.
[5] Aissa AH, Puzenatm E, Plassais A, Herrmann JM, Haehnel C, Guillard C. Characterization and photocatalytic performance in air of cementitious materials containing TiO_2. Case study of formaldehyde removal. Appl Catalytic B: Environ 2011;107:1–8.
[6] Pacheco-Torgal F, Jalali S. Nanotechnology: advantages and drawbacks in the field of construction and building materials. Constr Build Mater 2011;25:582–90.
[7] Diamanti MV, Ormellese M, Pedeferri M. Characterization of photocatalytic and superhydrophilic properties of mortars containing titanium dioxide. Cem Concr Res 2008;38:1349–53.
[8] Nazari A, Riahi S. TiO_2 nanoparticles effects on physical, thermal and mechanical properties of self compacting concrete with ground granulated blast furnace slag as binder. Energ Build 2011;43:995–1002.
[9] Sanchez F, Sobolov K. Nanotechnology in concrete – a review. Constr Build Mater 2010;24:2060–71.
[10] Jennings HM, Bullard JW. From electrons to infrastructure: engineering concrete from the bottom up. Cem Concr Res 2011;41:727–35.
[11] Lee BY, Kurtis KE. Influence of TiO_2 nanoparticles on early C3S hydration. J Am Ceram Soc 2010;93:3399–405.
[12] Vulic T, Hadnadjev M, Marinkovic-Neducin R. Structure and morphology of Mg–Al–Fe mixed oxides derived from layered double hydroxides. J Microsc 2008;232:634–8.
[13] Raki L, Beaudoin J, Alizadeh R, Makar J, Sato T. Cement and concrete nanoscience and nanotechnology. Materials 2010;3:918–42.
[14] Vulic T, Reitzmann A, Ranogajec J, Marinkovic-Neducin R. The influence of synthesis method and Mg–Al–Fe content on the thermal stability of layered double hydroxides. J Therm Anal Calorim 2012. http://dx.doi.org/10.1007/s10973-012-2230-9.
[15] Hadnadjev-Kostic M, Vulic T, Ranogajec J, Marinkovic-Neducin R, Radosavljevic-Mihajlovic A. Thermal and photocatalytic behaviour of Ti/LDH nanocomposites. J Therm Anal Calorim 2012. http://dx.doi.org/10.1007/s10973-012-2226-5.
[16] Sonawane RS, Kale BB, Dongare MK. Preparation and photocatalytic activity of Fe–TiO_2 thin films prepared by sol–gel dip coating. Mater Chem Phys 2004;85:52–7.
[17] SRPS EN 196-7:2010. Methods of testing cement – Part 7: methods of taking and preparing samples of cement.
[18] Tschirch J, Dillert R, Bahnemann D, Proft B, Biedermann A, Goer B. Photodegradation of methylene blue in water, a standard method to determine the activity of photocatalytic coatings. Res Chem Intermedia 2008;34:381–92.
[19] Hadnadjev M, Ranogajec J, Petrovic S, Markov S, Ducman V, Marinkovic-Neducin R. Design of self-cleaning TiO_2 coating on clay roofing tiles. Philos Mag 2010;90:2989–3002.
[20] Collins F, Lambert J, Duan WH. The influence of admixtures on the dispersion, workability, and strength of carbon nanotube-OPC paste mixtures. Cem Concr Comp 2012;34:201–7.
[21] Fernández Olmo I, Chacon E, Irabien A. Influence of lead, zinc, iron (III) and chromium (III) oxides on the setting time and strength development of Portland cement. Cem. Conc. Res. 2001;31:1213–9.
[22] Taylor HFW. Cement Chemistry. London: Academic Press; 1990.
[23] Tommaseo EC, Kersten M. Aqueous solubility diagrams for cementitious waste stabiliyation systems. 3. Mechanism of zinc immobilization by calcium silicate hydrate. Environ Sci Technol 2002;36:2919–25.

[24] Ziegler F, Gierè R, Johnson CA. Sorption mechanism of zinc to calcium silicate hydrate: sorption and microscopic investigation. Environ Sci Technol 2001;35:4556–61.
[25] Lowell S, Shields JE, Thomas MA, Thommes M. Characterization of porous solids and powders: surface area, pore size and density. Dordrecht/Boston/London: Kluwer Academic Publishers; 2004.
[26] Sing KSW, Everet DH, Haul RAW, Moscou L, Pierotti RA, Rouquerol J, et al. Reporting physisorption data for gas/solid systems with special reference to the determination of surface area and porosity. Pure Appl Chem 1985;57:603–19.